*Title Page

Validation of MRI to TRUS registration for HDR prostate brachytherapy

Running head title: MRI to TRUS registration for prostate brachytherapy

Eric Poulin[1,2], Karim Boudam[2], Csaba Pinter[3], Samuel Kadoury[4,5], Andras Lasso[3], Gabor Fichtinger[3], Cynthia Ménard[2,5,6 a)]

1. *Département de radio-oncologie et Axe Oncologie du Centre de recherche du CHU de Québec, CHU de Québec, 11 Côte du Palais, Québec, Canada, G1R 2J6*
2. *Département de radio-oncologie, CHUM, 1560 Rue Sherbrooke Est, Montréal, Canada, H2L 4M1*
3. *Laboratory for Percutaneous Surgery, School of Computing, Queen's University, 557 Goodwin Hall, Kingston, Canada, K7L 2N8*
4. *Department of Computer and Software Engineering, Polytechnique de Montréal, 2500 chemin de Polytechnique, Montréal, Canada, H3T 1J4*
5. *CRCHUM, Université de Montréal, 900 St-Denis, Montréal, QC, H2X 0A9*
6. *TECHNA Institute, 124-100 College St, Toronto, ON M5G 1L5*

[a)] Corresponding author:
Cynthia Ménard, MD
Département de radio-oncologie
CHUM
1560 Rue Sherbrooke Est,
Montréal, Canada, H2L 4M1
Tel: 1-514-890-8000 #24684
Fax: 1-514-412-7537
cynthia.menard@umontreal.ca

ABSTRACT

Purpose: The objective of this study was to develop and validate an open-source module for MRI to transrectal ultrasound (TRUS) registration to support tumor-targeted prostate brachytherapy.

Methods and Materials: In this study, fifteen patients with prostate cancer lesions visible on multiparametric MRI were selected for the validation. T2-weighted images with 1 mm isotropic voxel size and diffusion weighted images were acquired on a 1.5T Siemens. Three dimensional (3D) TRUS images with 0.5 mm slice thickness were acquired. The investigated registration module was incorporated in the open-source 3D Slicer platform and can compute rigid and deformable transformations. An extension of 3D Slicer, SlicerRT, allows import and export to DICOM-RT formats. For validation, similarity indices, prostate volumes and centroid positions were determined in addition to registration errors for common 3D points identified by an experienced radiation oncologist.

Results: The average time to compute the registration was 35±3 seconds. For the deformable and rigid registration respectively, Dice similarity coefficients were 0.93±0.01 and 0.87±0.05 while the 95% Hausdorff distance was 2.2±0.3 and 4.2±1.0 mm. MRI volumes obtained after the rigid and deformable registration were not statistically different ($p>0.05$) from reference TRUS volumes. For the deformable and rigid registration respectively, 3D distance error between centroid positions were 0.4±0.1 and 2.1±1.0 mm while registration errors between common points were 2.3±1.1 and 3.5±3.2 mm. Deformable registration was found significantly better ($p<0.05$) than rigid registration in all parameters.

Conclusions: An open-source MRI to TRUS registration platform was validated for integration in the brachytherapy workflow.

Key words: HDR brachytherapy, registration, MRI, ultrasound, prostate, open source

INTRODUCTION

Long-term disease control for prostate cancer patients can be achieved using high dose rate (HDR) brachytherapy [1,2] with conventional techniques treating the whole gland. However, such an approach may limit the efficacy of radiotherapy as escalation of dose will be limited by the tolerance of adjacent organs at risk [3]. Pathology studies suggest that in many cases a dominant cancer focus may exist within the gland and could be at the epicenter of recurrence post treatment [4,5]. Strategies to identify and intensify treatment to dominant intraprostatic lesions (GTV) are therefore needed, and MRI demonstrates high performance in addressing this need [6,7]. Multiparametric MRI [8,9] has been integrated in the clinic to identify the GTV in order to boost or target intraprostatic lesions [10,11]. Several recent studies were performed to investigate the feasibility of dose escalation and focal brachytherapy using mpMRI to define GTVs [12–16].

However, a significant number of programs are using transrectal ultrasound (TRUS) as their treatment planning modality due to its low cost, easy accessibility and real time capability. The current clinical procedures, based on ultrasound images, can't identify the position of the GTV [17]. Therefore, a spatial registration is needed between MRI and TRUS images in order to accurately position the GTV. Adequate registration between MRI and TRUS would allow dose escalation or focal brachytherapy using an ultrasound technique. On the other hand, most rigid registration algorithms rely on similar prostate shape [18]; which is often inadequate. In fact, the prostate shape is often different between TRUS and MRI images; a transrectal probe is used to obtain TRUS images while MRI images are usually obtained several days before TRUS images, with or without an endorectal coil. In brachytherapy, there is currently no commercially available MRI to TRUS deformable registration algorithm to correct for this difference in prostate shape.

Several commercial MRI to TRUS registration systems are available for biopsy patients [19], however they were not adapted to prostate brachytherapy and they have several issues. In fact, most commercial MRI/TRUS fusion products implement linear registration only [19]. In addition, they are typically used as a black box and do not allow the export of the registration results [18]. MRI can be segmented in advance of the brachytherapy procedure, therefore a registration algorithm based on the contours would be a feasible approach. RaySearch Laboratories do offer a contour-based deformable registration algorithm MORFEUS [20], however accessibility to the system is limited and there is no publication that specifically validates the algorithm for MRI to TRUS prostate registration to date.

The goal of the study was to develop and validate an open-source module for MRI to TRUS registration to support tumor-targeted prostate brachytherapy. The module was implemented in the 3D Slicer medical image visualization and analysis software platform [21].

MATERIALS AND METHODS

Clinical Data

Fifteen patients who underwent HDR brachytherapy with confirmed prostate cancer and lesions visible on MRI were selected for the validation. T2-weighted 3D variable-flip-angle Turbo Spin Echo images with 1 mm isotropic voxel, ADC maps (b-value = 50, 500 and 1000 s/mm^2) and extrapolated diffusion weighted images with b-value = 1400 s/mm^2 were acquired on a 1.5T Siemens Aera Magnetom (Siemens Healthcare, Erlangen, Germany), using surface coils, for prostate and GTV contouring. 3D TRUS images, with 0.5 mm thick slices, were obtained with Oncentra Prostate (OcP) system v4.2 (Elekta Brachytherapy, Veneedal, The Netherlands) using BK Flex Focus 400 and the transrectal probe 8848 (BK Ultrasound, Peabody, United States). MRI contouring was performed at least one day prior to the procedure on the Varian Eclipse planning station (Varian Medical Systems, Palo Alto, United States) while TRUS contours, prior to catheter placement, were obtained on OcP during the HDR brachytherapy procedure.

Registration

The registration software tool is available as a module of the open-source 3D Slicer platform [21]. Figure 1 shows the MRI/TRUS registration module within the 3D Slicer environment. The user needs to install the extension Segment Registration through the 3D Slicer extension manager and the module name is Prostate MRI/US Contour Propagation. The SlicerProstate and SlicerRT [22] extensions are utilized by the new modules for the data management and registration steps. The validated BRAINSFit algorithm was used for the registration [23]. The proposed module is also based on a validated registration method based on distance maps [18]. Before the registration step, 3D TRUS volumes were resampled to the resolution of T2-weighted MRI volumes (1 mm). Briefly, the rigid registration method uses an iterative closest point method on the prostate surface meshes [24] to align both prostate contour. Consequently, the centroid of the reference and moving image should closely match in the same coordinate space. The deformable registration [18] is performed after the initial rigid registration. First, an affine registration is performed. Second, a B-spline regularization is executed to elastically align the binary 3D label maps. The proposed module, combined with SlicerRT, allows DICOM-RT structures to be imported. Furthermore, the module permits the conversion of planar contours, generated by the treatment planning system, to label maps; where, for example, a label map volume can be defined as a 3D scalar volume node where each voxel is a number indicating the type of tissue at that location. This representation allows the efficient handling of the different representations of the segmentation. In addition, contours transformed from rigid and deformable transformations can be exported in RT structures, which are compatibles in a treatment planning system. The transformed contour (defined here as either *rigid and deform contours*) is converted to the original 3D TRUS resolution. Several metrics were added to the module to provide a fast and accurate method to evaluate the registration results. Similarity metrics such as Hausdorff distance [25] and Dice similarity coefficient [26] are computed in addition to volume and centroid measures. In addition, the user can identify landmarks or common points on both modalities and calculate the Target Registration Errors (TRE), which will be used for validation.

End-to-end validation

The end-to-end validation of the module, for focal or dose escalation HDR prostate brachytherapy, was performed in three steps. First, the precision and accuracy of both rigid and deformable registration methods were evaluated. Second, a clinical workflow is proposed to perform tumor-targeted HDR brachytherapy. Third, the proposed workflow was implemented prospectively.

To evaluate the precision and accuracy of both rigid and deformable registration methods, prostate contours were delineated by an experienced radiation oncologist (CM) on both MRI and TRUS images for the fifteen patients. In addition, naturally occurring common points were also identified on TRUS and MRI registered images. Metrics such as the Dice similarity coefficient and Hausdorff distance indices were calculated to validate the registration. Specifically, maximum, 95% and mean Hausdorff distance metrics were calculated. In addition, volumes were compared and TREs were calculated for the prostate centroid and common points. The analysis was based on the AAPM report 132 [27].

Fig. 2 shows the proposed clinical workflow to perform tumor-targeted prostate HDR brachytherapy based on TRUS planning and MRI GTV contouring. Briefly, MRI images are obtained one week before the implant to allow sufficient time to contour the GTV and the prostate. MRI patient scans were acquired under specific brachytherapy guidelines to reproduce rectum and bladder filling states; this allows a closer representation of the prostate the day of the implant. For validation purposes and the identification of common points, a TRUS volume is acquired prior to needle insertion and the prostate is contoured. The TRUS contour is imported into 3D Slicer, and a registration is carried out between the MRI and TRUS prostate; the MRI prostate rigid and/or deformable transformation is applied to the MRI GTV. The transformed contours are exported in DICOM-RT format and imported back into the treatment planning system. Catheter insertion can be initiated while the registration is being calculated. The imported RT structure can then serves as guidance information to plan needle insertion to obtain optimal coverage of the GTV. At the end of the insertion, a final 3D TRUS scan is performed to contour the prostate, as the shape can change after needle insertion. A final registration is accomplished between the prostate post-implant and the MRI contours, and the transformed MRI contours are imported back into the treatment planning system. Finally, the catheter reconstruction is performed before the planning and treatment can be completed. The proposed workflow was tested prospectively on seven patients of the cohort, in parallel to the standard practice, to evaluate the clinical impact of the proposed methods on the overall efficiency of the procedure. The software was installed on a Dell Precision T7500 machine with Intel Xeon CPU E5620 2.4 GHz with 6 GB of RAM.

Statistical analysis

GraphPad Prism 5 (GraphPad Software, La Jolla, CA, USA) was used to perform all statistical analyses. The differences were evaluated using a paired student *t*-test and a one-way Anova, using Dunnett's multiple comparisons test. A p value < 0.05 (*) was considered as statistically significantly different ($p < 0.01$: **; $p < 0.001$: ***) . The Tukey method was used to make Box-and-whisker plots.

RESULTS

Out of the fifteen available patients in the cohort, fourteen were available for analysis. One patient was excluded due to an inadequate fusion. Fig. 3 and 4 show a representative registration between MRI (blue) and TRUS (red) contours for rigid and deformable registration, respectively. In the posterior portion of the prostate near the rectum, the deformed contour closely matches the reference TRUS prostate, while the rigid contour extends into the rectum. In the sagittal plane of Fig. 3 and on the coronal plane of Fig. 1, a TRUS cyst was identified that closely matches its position in the deformed MRI volume. Conversely, the rigid MRI volume in Fig. 4 shows the cyst with an offset compared to its position in the TRUS volume. The deformable registration allows a better representation of the prostate at the time of brachytherapy. Fig. 5 shows the results of the deformable registration for the patient dataset that was excluded from the analysis. The rectum was distended on the day of the MRI and the resulting deformation was not biologically plausible, with an s shape on the coronal image.

Fig. 6 shows a) the reference 3D TRUS volume as well as the rigid and deform MRI volumes, the comparison between rigid and deform registrations for b) Dice similarity coefficient and c) maximum, mean and 95% Hausdorff distance. Rigid and deform MRI volumes (38.8 ± 10.2, 39.5 ± 10.5 cm^3) were not statistically different ($p > 0.05$; One-way Anova Dunnett's multiple comparisons test) from reference TRUS volumes (38.5 ± 10.3 cm^3). Dice similarity coefficients were found significantly better ($p < 0.001$; *t*-test) using deformable registration (mean: 0.93 ± 0.01) compared to rigid registration (mean: 0.87 ± 0.04). The average 95% Hausdorff distance is

4.2±1.0 mm and 2.2±0.3 mm for rigid and deformable registration methods, respectively. Hausdorff distance values were found to be significantly better for the deformable registration method ($p < 0.0001$; *t*-test). Fig. 7 shows 3D distance error between centroid positions. The deform MRI volume centroid, with a 3D error of 0.4 ± 0.1 mm, is statistically better ($p < 0.001$; *t*-test) than the rigid MRI volume, with an error of 2.1 ± 1.0 mm. Fig. 8 shows TRE found between common points identified in TRUS and rigid or deformable MRI images. The mean deformable registration TRE was found to be significantly better ($p < 0.05$; *t*-test) than the rigid registration (3.5±3.2 mm and 2.3±1.1 mm for the rigid and deform registration, respectively). The computation time to perform the deformable registration is 35 ± 3 seconds. The complete registration step, defined in Fig. 2, is performed in a clinically acceptable time, however the initial registration on the pre-implant TRUS image reduce the efficiency of the workflow.

DISCUSSION

The developed open-source module for MRI to TRUS registration offers quality metrics such as the Dice similarity coefficient and Hausdorff distance in addition to volume, centroid comparison and TRE calculation between fiducials to assess the accuracy of the registration for each patient. In addition, it allows to import and export RT structures for use in brachytherapy therapy planning software. In the present study, transformed RT structures were successively imported into OcP treatment planning system, a requirement for brachytherapy procedures. The registration workflow, defined in Fig. 2, can be performed in a clinically acceptable time. However, the initial registration with the pre-implant TRUS image reduce the efficiency of the procedure with no real clinical gain, for this reason the registration is now only performed with the TRUS image planning volume. Note that the initial registration with the pre-implant TRUS was needed for the validation and to identify common points with the MRI, which are no longer discernible after catheter placement. Therefore, the MRI to TRUS registration is feasible in a clinical setting.

The deformable registration was found to be significantly better than rigid registration in terms of Dice similarity coefficient, Hausdorff distance, centroid and common points positions ($p < 0.05$). The rigid and deform MRI volumes were not statistically different from the reference TRUS volume ($p > 0.05$). Fig. 3-4 showed that the deformable registration allows a better representation of the prostate at the time of brachytherapy than the rigid registration, as it can correct for the TRUS probe deformation. The 95% Haussdorff distance and common points TRE suggest an accuracy of approximately 3.5 mm and 2 mm for the rigid and deformable registration methods, respectively. The deformable registration was successful in 14 patients out of 15. The patient that was removed from the analysis had a distended rectum on the day of the MRI. The registration results from that patient yielded a Dice similarity coefficient of 0.88, however it was impossible to identify common points in the prostate as the deformation vector field was too important and biologically implausible. Therefore, it is important to evaluate the deformed images and not only to indices such as Dice similarity coefficient and Haussdorff distance [27]. MRI to TRUS registration helped to delineate the prostate on TRUS as was shown by Reynier *et al.* [28], particularly in the apex and base region.

In comparison with commercial systems that support biopsy [19], the open-source registration method developed in the present study allows both rigid and deformable registration. In addition, it can import and export DICOM-RT structures, a requirement for brachytherapy procedures. The current deformable registration method offers increased levels of accuracy compared to the initial version published by Federov *et al.* in 2015 [18], which showed TRE of approximately 3 mm compared to 2 mm here. Recently, several papers [28–32] were published on deformable registration with TRE ranging from 2.4 to 3.4 mm, which demonstrates that the authors registration approach is consistent with published reports. The 1 mm isotropic resolution of the MRI could be partly responsible for the improved performance of the algorithm.

CONCLUSIONS

In conclusion, an open-source MRI to TRUS registration platform was validated for tumor-targeted prostate brachytherapy. The registration workflow was found to be sufficiently efficient for use in the clinical workflow. The deformable registration algorithm was found to significantly improve results compared to the rigid registration methods, and can correct for prostate deformation induced by probe pressure. The deformable registration algorithm contributes to an uncertainty of 2 mm on the GTV. This study demonstrates that the deformable registration is sufficiently accurate and precise for use in tumor-targeted HDR prostate brachytherapy treatment.

ACKNOWLEDGMENTS

We thank Jean-François Pambrun for his assistance in the study. This research has been funded in part by Institut du cancer de Montréal (ICM).

REFERENCES

[1] Pieters BR, de Back DZ, Koning CCE, Zwinderman AH. Comparison of three radiotherapy modalities on biochemical control and overall survival for the treatment of prostate cancer: A systematic review. Radiother Oncol 2009;93:168–73. doi:10.1016/j.radonc.2009.08.033.

[2] Boladeras A, Santorsa L, Gutierrez C, Martinez E, Pera J, Pino F, et al. External beam radiotherapy plus single-fraction high dose rate brachytherapy in the treatment of locally advanced prostate cancer. Radiother Oncol 2014;112:227–32. doi:10.1016/j.radonc.2014.07.013.

[3] Viani GA, Stefano EJ, Afonso SL. Higher-Than-Conventional Radiation Doses in Localized Prostate Cancer Treatment: A Meta-analysis of Randomized, Controlled Trials. Int J Radiat Oncol • Biol • Phys 2009;74:1405–18. doi:10.1016/j.ijrobp.2008.10.091.

[4] Mouraviev V, Villers A, Bostwick DG, Wheeler TM, Montironi R, Polascik TJ. Understanding the pathological features of focality, grade and tumour volume of early-stage prostate cancer as a foundation for parenchyma-sparing prostate cancer therapies: active surveillance and focal targeted therapy. BJU Int 2011;108:1074–85. doi:10.1111/j.1464-410X.2010.10039.x.

[5] Pucar D, Hricak H, Shukla-Dave A, Kuroiwa K, Drobnjak M, Eastham J, et al. Clinically Significant Prostate Cancer Local Recurrence After Radiation Therapy Occurs at the Site of Primary Tumor: Magnetic Resonance Imaging and Step-Section Pathology Evidence. Int J Radiat Oncol • Biol • Phys 2007;69:62–9. doi:10.1016/j.ijrobp.2007.03.065.

[6] Dickinson L, Ahmed HU, Allen C, Barentsz JO, Carey B, Futterer JJ, et al. Magnetic Resonance Imaging for the Detection, Localisation, and Characterisation of Prostate Cancer: Recommendations from a European Consensus Meeting. Eur Urol 2011;59:477–94. doi:10.1016/j.eururo.2010.12.009.

[7] Blanchard P, Ménard C, Frank SJ. Clinical use of magnetic resonance imaging across the prostate brachytherapy workflow. Brachytherapy 2017;16:734–42. doi:10.1016/j.brachy.2016.11.012.

[8] de Rooij M, Hamoen EHJ, Fütterer JJ, Barentsz JO, Rovers MM. Accuracy of Multiparametric MRI for Prostate Cancer Detection: A Meta-Analysis. Am J Roentgenol 2014;202:343–51. doi:10.2214/AJR.13.11046.

[9] Hegde JV, Mulkern RV, Panych LP, Fennessy FM, Fedorov A, Maier SE, et al. Multiparametric MRI of prostate cancer: An update on state-of-the-art techniques and their performance in detecting and localizing prostate cancer. J Magn Reson Imaging 2013;37:1035–54. doi:10.1002/jmri.23860.

[10] Bauman G, Haider M, Van der Heide UA, Ménard C. Boosting imaging defined dominant prostatic tumors: A systematic review. Radiother Oncol 2013;107:274–81. doi:10.1016/j.radonc.2013.04.027.

[11] Venkatesan AM, Stafford RJ, Duran C, Soni PD, Berlin A, McLaughlin PW. Prostate magnetic resonance imaging for brachytherapists: Diagnosis, imaging pitfalls, and post-therapy assessment. Brachytherapy 2017;16:688–97. doi:10.1016/j.brachy.2016.12.012.

[12] Crook J, Ots A, Gaztañaga M, Schmid M, Araujo C, Hilts M, et al. Ultrasound-planned high-dose-rate prostate brachytherapy: Dose painting to the dominant intraprostatic lesion. Brachytherapy 2014;13:433–41. doi:10.1016/j.brachy.2014.05.006.

[13] Vigneault E, Mbodji K, Racine L-G, Chevrette E, Lavallée M-C, Martin A-G, et al. Image-guided high-dose-rate brachytherapy boost to the dominant intraprostatic lesion using multiparametric magnetic resonance imaging including spectroscopy: Results of a prospective study. Brachytherapy 2016;15:746–51. doi:10.1016/j.brachy.2016.09.004.

[14] Mason J, Al-Qaisieh B, Bownes P, Wilson D, Buckley DL, Thwaites D, et al. Multi-parametric MRI-guided focal tumor boost using HDR prostate brachytherapy: A feasibility study. Brachytherapy 2014;13:137–45. doi:10.1016/j.brachy.2013.10.011.

[15] Peach MS, Trifiletti DM, Libby B. Systematic Review of Focal Prostate Brachytherapy and the Future Implementation of Image-Guided Prostate HDR Brachytherapy Using MR-Ultrasound Fusion. Prostate Cancer 2016;2016:1–13. doi:10.1155/2016/4754031.

[16] Kollmeier MA, Zelefsky M, McBride S. Magnetic resonance imaging-based salvage brachytherapy: Moving toward a focal paradigm. Brachytherapy 2017;16:770–7. doi:10.1016/j.brachy.2017.02.009.

[17] Frank SJ, Mourtada F, Crook J, Ménard C. Use of magnetic resonance imaging in low-dose-rate and high-dose-rate prostate brachytherapy from diagnosis to treatment assessment: Defining the knowledge gaps, technical challenges, and barriers to implementation. Brachytherapy 2017;16:672–8. doi:10.1016/j.brachy.2017.01.014.

[18] Fedorov A, Khallaghi S, Sánchez CA, Lasso A, Fels S, Tuncali K, et al. Open-source image registration for MRI–TRUS fusion-guided prostate interventions. Int J Comput Assist Radiol Surg 2015;10:925–34. doi:10.1007/s11548-015-1180-7.

[19] Logan JK, Rais-Bahrami S, Turkbey B, Gomella A, Amalou H, Choyke PL, et al. Current Status of MRI and Ultrasound Fusion Software Platforms for Guidance of Prostate Biopsies. BJU Int 2014;114:641–52. doi:10.1111/bju.12593.

[20] Brock KK, Nichol AM, Ménard C, Moseley JL, Warde PR, Catton CN, et al. Accuracy and sensitivity of finite element model-based deformable registration of the prostate. Med Phys 2008;35:4019–25. doi:10.1118/1.2965263.

[21] Fedorov A, Beichel R, Kalpathy-Cramer J, Finet J, Fillion-Robin J-C, Pujol S, et al. 3D Slicer as an Image Computing Platform for the Quantitative Imaging Network. Magn Reson Imaging 2012;30:1323–41. doi:10.1016/j.mri.2012.05.001.

[22] Pinter C, Lasso A, Wang A, Jaffray D, Fichtinger G. SlicerRT: Radiation therapy research toolkit for 3D Slicer. Med Phys 2012;39:6332–8. doi:10.1118/1.4754659.

[23] Jonhson H, Harris G, Williams K. BRAINSFit: Mutual Information Registrations of Whole-Brain 3D Images, Using the Insight Toolkit. Insight J 2007.

[24] Moradi M, Janoos F, Fedorov A, Risholm P, Kapur T, Wolfsberger LD, et al. Two Solutions for Registration of Ultrasound to MRI for Image-Guided Prostate Interventions. Conf Proc Annu Int Conf IEEE Eng Med Biol Soc IEEE Eng Med Biol Soc Conf 2012;2012. doi:10.1109/EMBC.2012.6346134.

[25] Hausdorff F. Grundzüge der Mengenlehre. Leipzig Viet; 1914.

[26] Dice LR. Measures of the Amount of Ecologic Association Between Species. Ecology 1945;26:297–302. doi:10.2307/1932409.

[27] Brock KK, Mutic S, McNutt TR, Li H, Kessler ML. Use of Image Registration and Fusion Algorithms and Techniques in Radiotherapy: Report of the AAPM Radiation Therapy Committee Task Group No. 132. Med Phys 2017.

[28] Reynier C, Troccaz J, Fourneret P, Dusserre A, Gay-Jeune C, Descotes J-L, et al. MRI/TRUS data fusion for prostate brachytherapy. Preliminary results. Med Phys 2004;31:1568–75. doi:10.1118/1.1739003.

[29] Onofrey JA, Staib LH, Sarkar S, Venkataraman R, Nawaf CB, Sprenkle PC, et al. Learning Non-rigid Deformations for Robust, Constrained Point-based Registration in Image-Guided MR-TRUS Prostate Intervention. Med Image Anal 2017;39:29–43. doi:10.1016/j.media.2017.04.001.

[30] Hu Y, Ahmed HU, Taylor Z, Allen C, Emberton M, Hawkes D, et al. MR to ultrasound registration for image-guided prostate interventions. Med Image Anal 2012;16:687–703. doi:10.1016/j.media.2010.11.003.

[31] Mayer A, Zholkover A, Portnoy O, Raviv G, Konen E, Symon Z. Deformable registration of trans-rectal ultrasound (TRUS) and magnetic resonance imaging (MRI) for focal prostate brachytherapy. Int J Comput Assist Radiol Surg 2016;11:1015–23. doi:10.1007/s11548-016-1380-9.

[32] Sparks R, Bloch BN, Feleppa E, Barratt D, Madabhushi A. Fully Automated Prostate Magnetic Resonance Imaging and Transrectal Ultrasound Fusion via a Probabilistic Registration Metric. Proc SPIE-- Int Soc Opt Eng 2013;8671:86710A. doi:10.1117/12.2007610.

Figure 1 : Screen capture showing the 3D Slicer environment as well as the registration module.

Figure 2 : New clinical workflow proposed to perform tumor-targeted prostate HDR brachytherapy.

Figure 3 : Representation of the deformed MRI volume on the top row and the TRUS volume on the bottom row. Arrows show regions of interest (a cyst and the rectum), the reference TRUS prostate volume is outline in red while the MRI-deformed GTV and prostate are in dark red and blue, respectively.

Figure 4 : Representation of the rigidly transformed MRI volume on the top row and the TRUS volume on the bottom row. Arrows show regions of interest (a cyst and the rectum), the reference TRUS prostate volume is outline in red while the MRI-deformed GTV and prostate are in dark red and blue respectively.

Figure 5 : Results of the failed deformable registration for the patient that was excluded from the analysis. The deformed MRI volume is shown on the top row and the TRUS volume on the bottom row.

Figure 6 : Results obtained with the open-source registration method. a) Volume comparison between the reference TRUS volume and the rigid as well as the deform volumes. Comparison between rigid and deform registration for b) Dice similarity coefficient and c) maximum, mean and 95% Hausdorff distance values.

Figure 7 : 3D distance errors calculated for the centroid in both rigid and deformable approaches.

Figure 8 : TRE calculated for the fiducials identified in the 3D TRUS volume as well as in both rigid and deform MRI volumes.

Figure 1

Click here to download high resolution image

Figure 2
Click here to download high resolution image

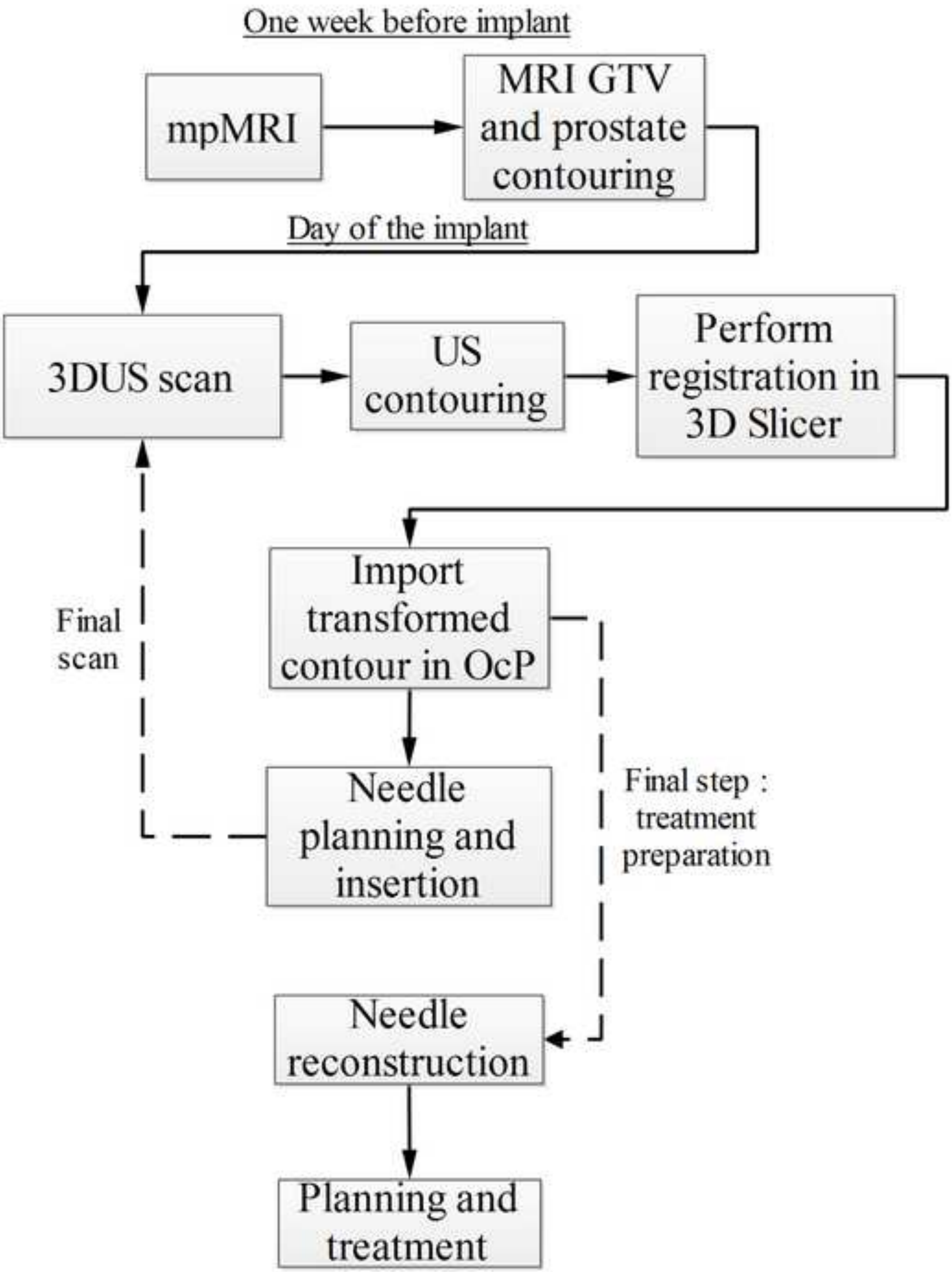

Figure 3

Click here to download high resolution image

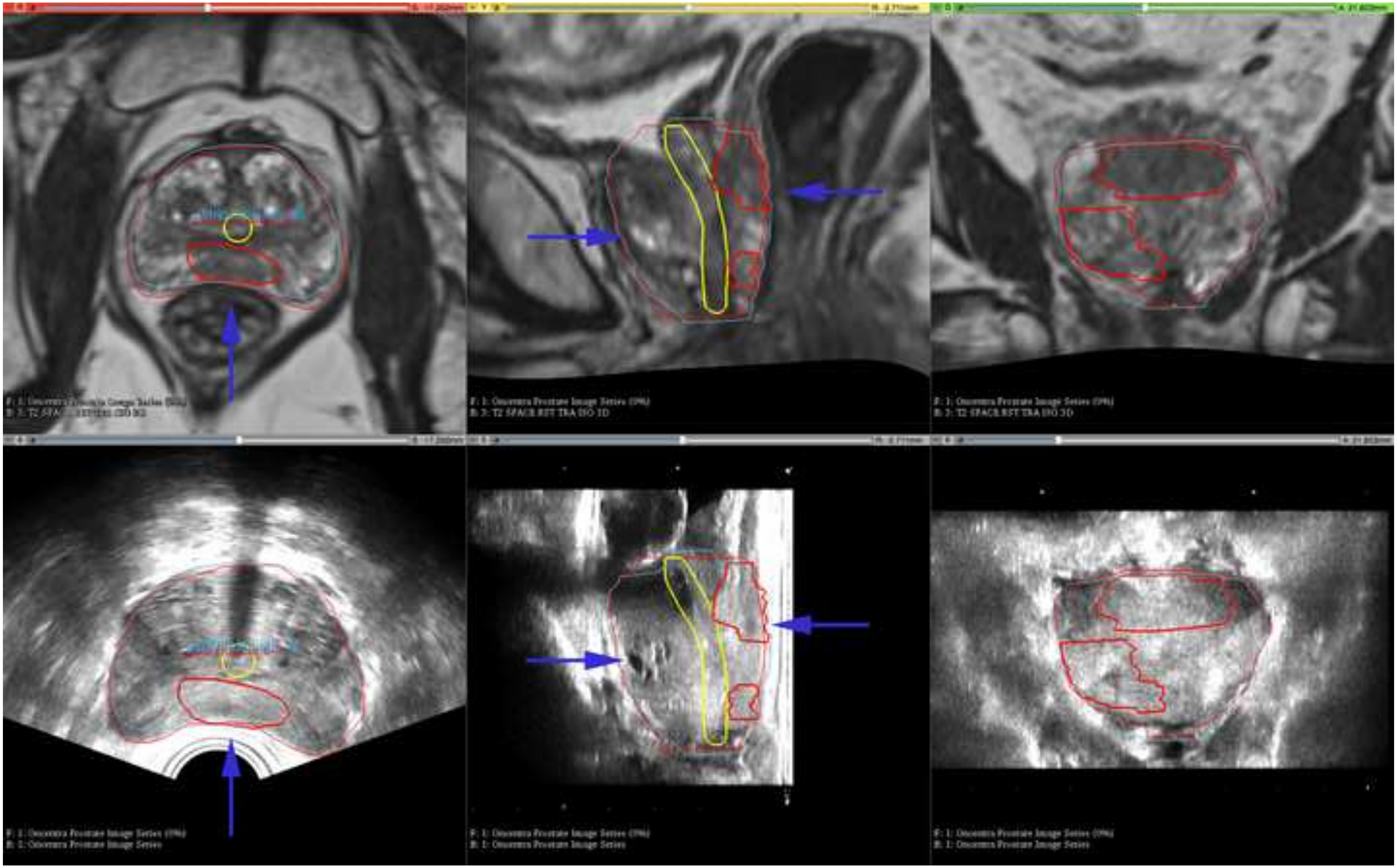

Figure 4
Click here to download high resolution image

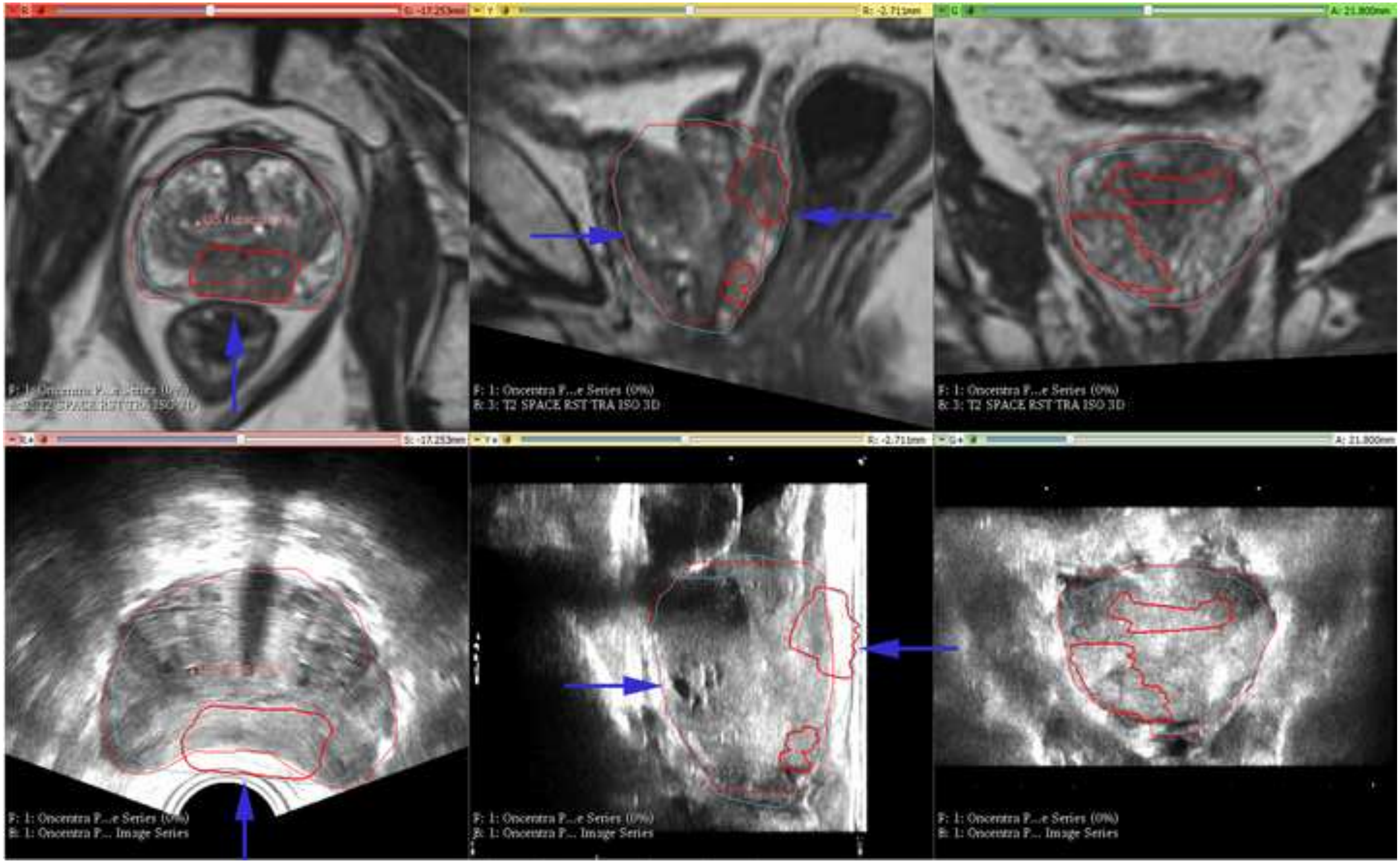

Figure 5

Click here to download high resolution image

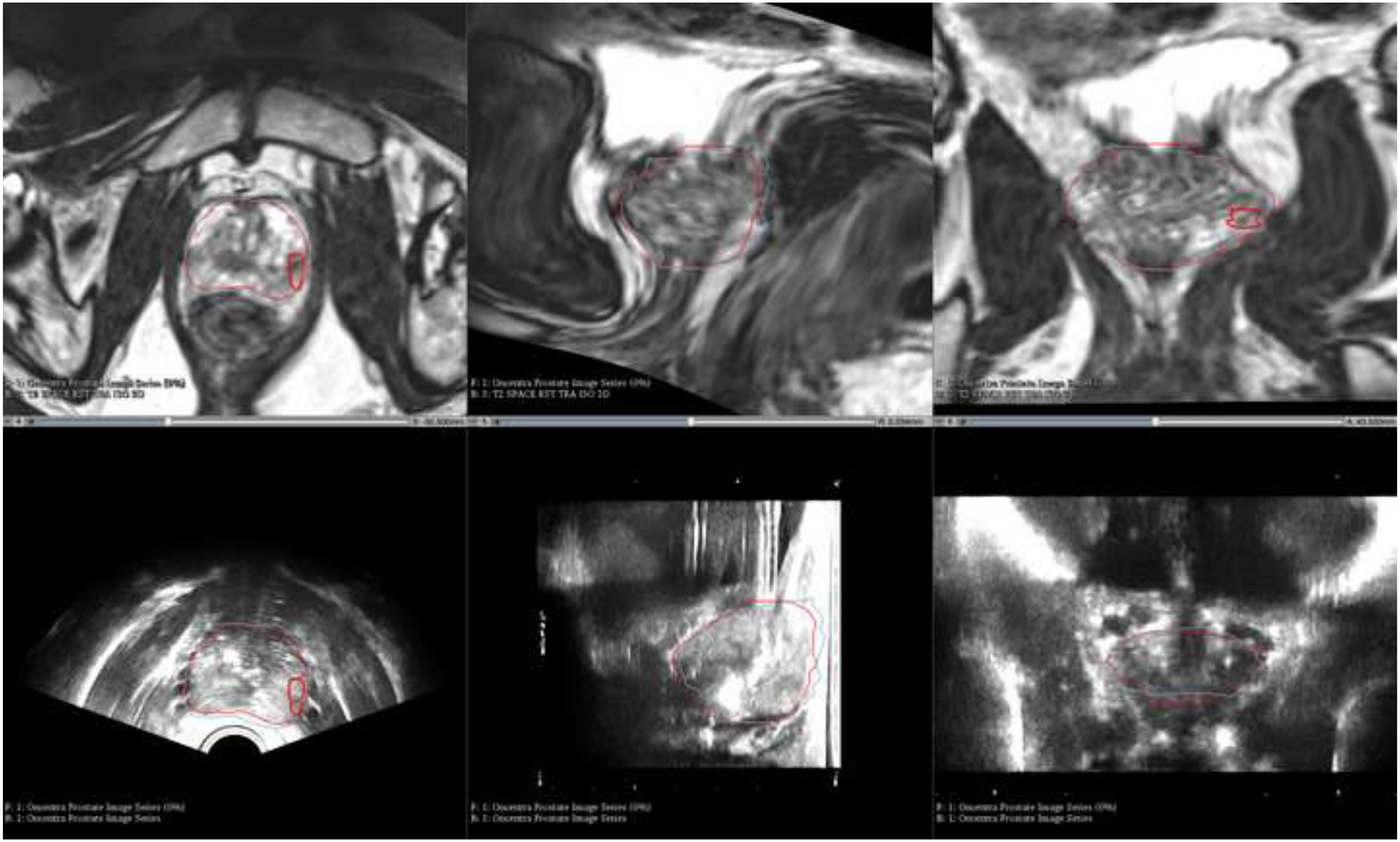

Figure 6
Click here to download high resolution image

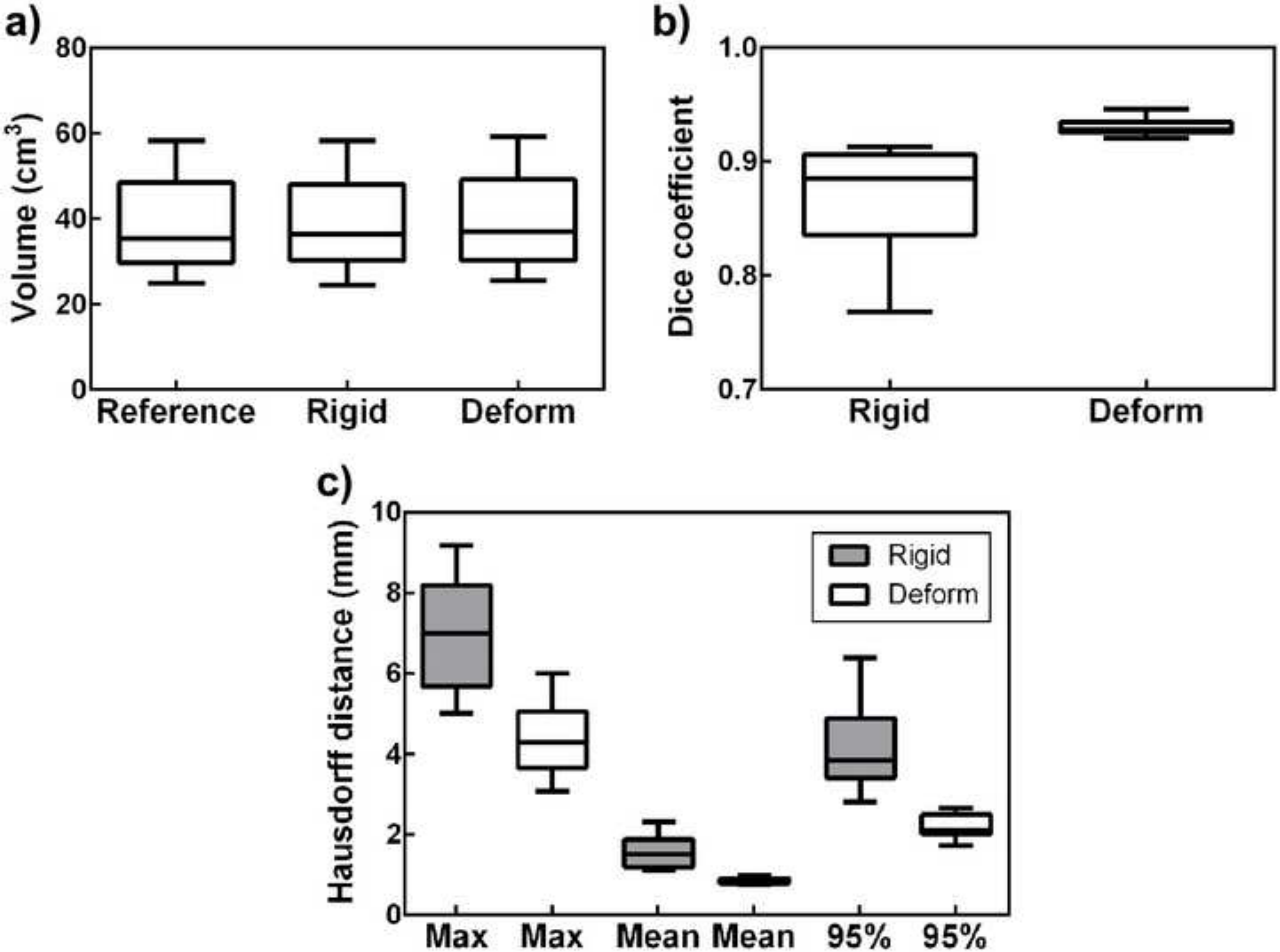

Figure 7
Click here to download high resolution image

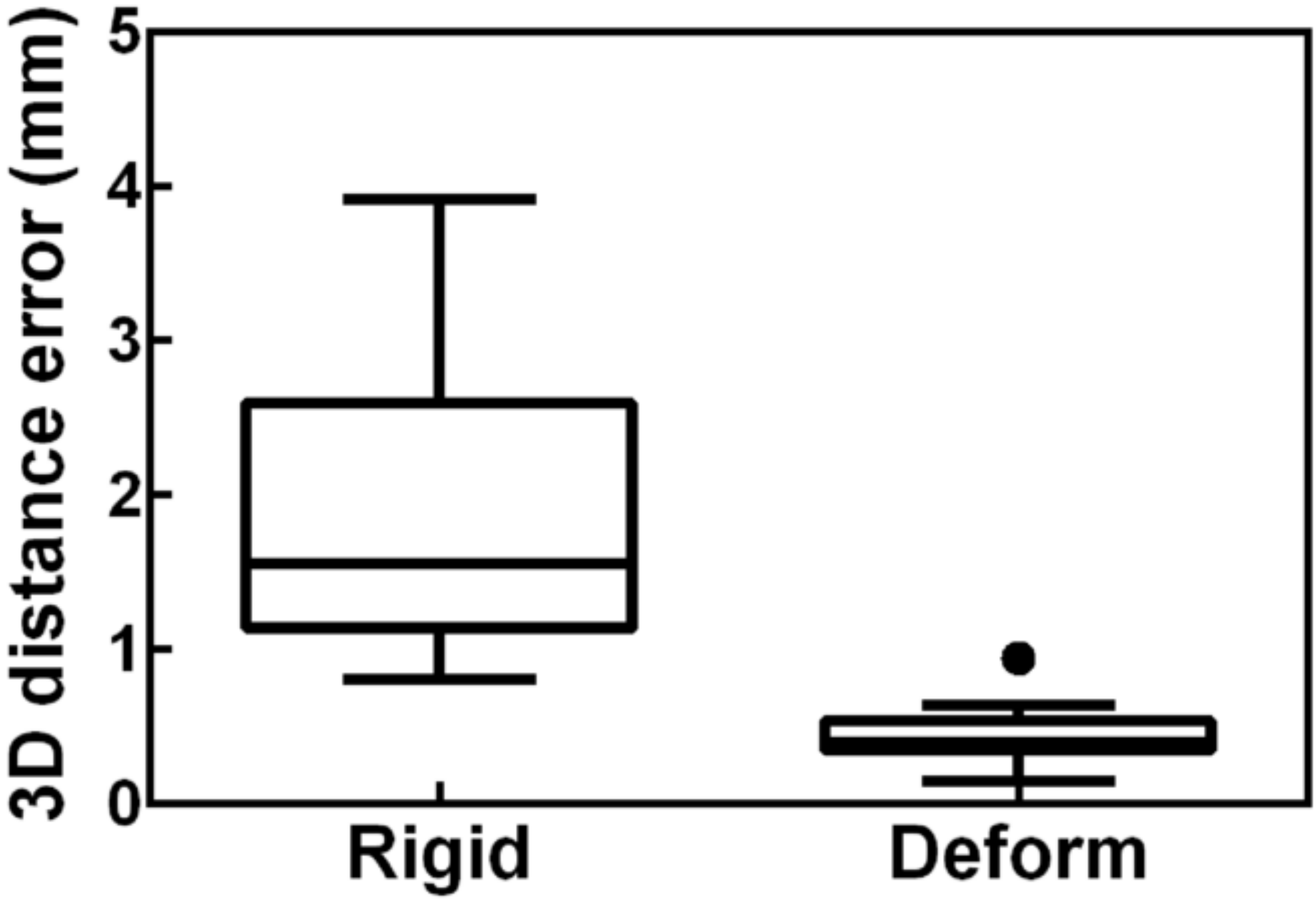

Figure 8
Click here to download high resolution image

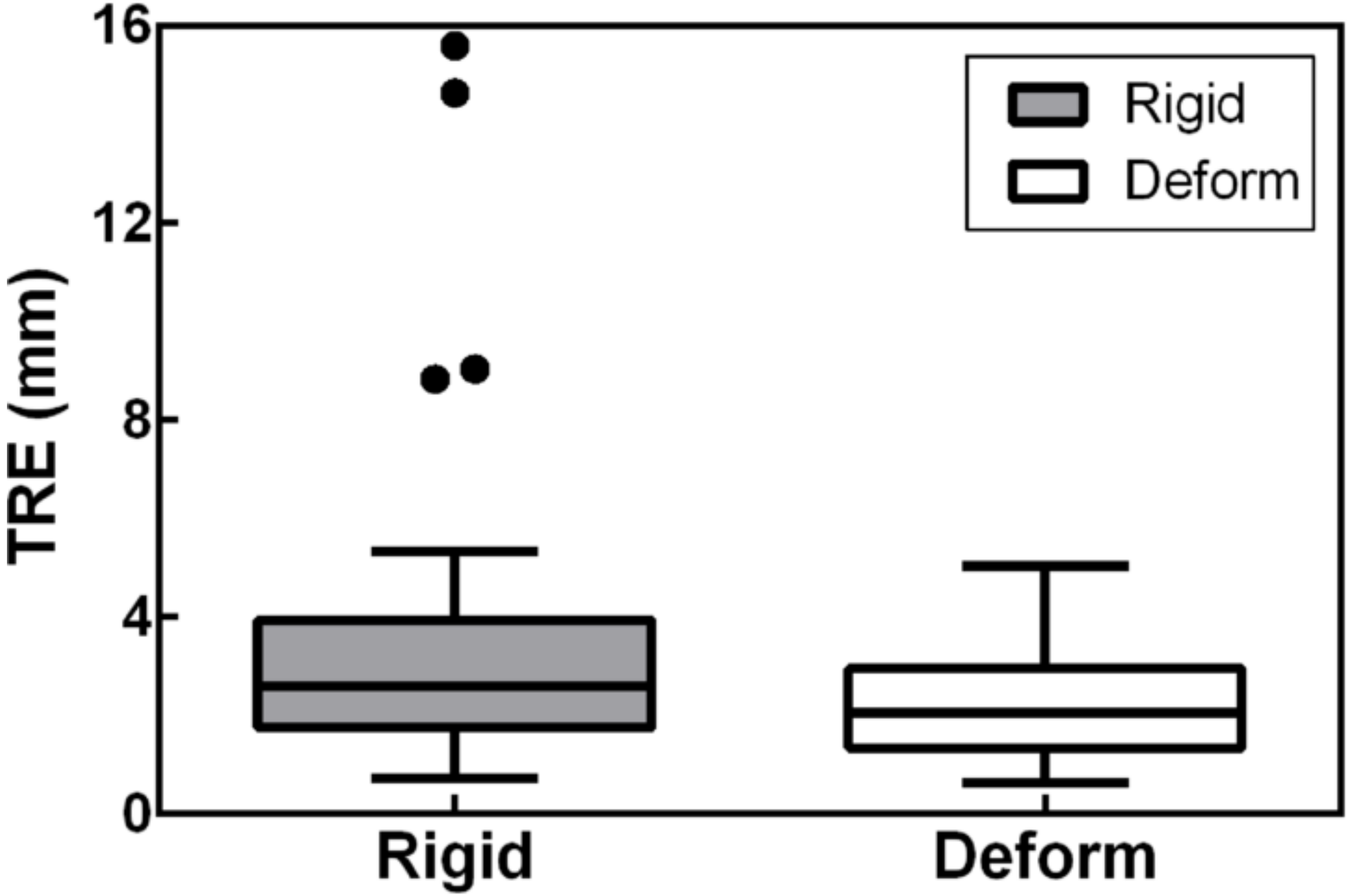

LIST OF ABBREVIATIONS

TRUS:	Transrectal ultrasound
3D :	Three dimensional
MRI :	Magnetic Resonance Imaging
HDR :	High dose rate
GTV :	Gross tumor volume or here dominant intraprostatic lesions
OcP :	Oncentra Prostate
TRE :	Target Registration Errors